NURETH14-374

THE EFFECT OF BUBBLE-INDUCED TURBULENCE AND THE BUBBLE SIZE ON THE INTERFACIAL AREA TRANSPORT IN GAS-LIQUID TWO-PHASE FLOW

Van Thai NGUYEN^{1,2}, Byoung-Uhn BAE², Dong Jin EUH², and Chul-Hwa SONG*^{1,2}

¹ University of Science and Technology, Yuseong, Daejeon, Rep. of KOREA

² Korea Atomic Energy Research Institute, Yuseong, Daejeon, Rep. of KOREA

* Corresponding author: Dr. C-.H. Song (chsong@kaeri.re.kr)

Abstract

In the present work, two common modeling concepts taking into account of the influence of bubbles on the turbulence of liquid phase were implemented in the EAGLE code and assessed against Hibiki's experiment data [1]. The EAGLE (Elaborated Analysis of Gas-Liquid Evolution) code has been developed at KAERI based on the two-fluid model for a multi-dimensional analysis of two-phase flow with the implementations of non-drag force, standard k-ɛ turbulence model, and the interfacial area transport equation [2],[3]. In order to investigate the bubble size effect on two-phase flow evolution and to provide a data set for developing the physical models to describe the bubble-induced turbulence effect and also for validating the EAGLE code, a series of local parameter measurements as well as visualization tests were conducted in air-water vertical-upward flow condition in which the initial bubble size is controlled by a specially designed bubble generator. The numerical and experimental results are compared, analyzed and discussed in this paper.

Introduction

The introduction of interfacial area transport equation (IATE) has been proposed [4], [5] in order to replace the traditional flow regime maps and regime transition criteria in the two-phase flow analysis codes. Although the basic frame and source terms of the IATE have been established and modelled, it still needs more efforts to improve the performance of modelling source terms for local and/or systematic dynamic behaviour based on the phenomenological understandings [6]. In bubbly flows without phase changes, the development of physical models for bubble break-up and coalescence requires the consideration of bubble size distribution as well as the dynamic interaction between bubbles or bubble and liquid turbulence. Literature researches have shown the unsatisfying results regarding the simulation of the bubble coalescence and break-up [7], [8], [9]. One of the reasons may come from the shortcoming on the calculation of the local turbulent kinetic energy k and its dissipation rate ε because local bubble coalescence and break-up rates strongly depend upon these parameters. The standard k- ε turbulence model has proven successful for the description of single-phase turbulent flows for many industrial applications and extended to two-phase flow applications. However, the influence of bubbles on turbulence has to be considered and modelled correctly.

The EAGLE code has been developed based on the two-fluid model and aimed for a multi-dimensional analysis of two-phase flow with the implementations of non-drag force, standard k-ɛ turbulence model, and the IATE. The performance of EAGLE has been validated

for sub-cooled boiling flows and showed good agreement with experimental data [2], [3]. This paper focuses on the adiabatic two-phase flow conditions in which the bubble-induced turbulence models taking into account the influence of bubbles on liquid turbulence are implemented in EAGLE code. The numerical results are compared, analysed against the experimental data of Hibiki et al. [1].

Recent trend in open literature shows the coupling of the population balance equation to CFD code to model a poly-dispersed bubbly flow. A fixed bubble size model might not be suitable for predicting correctly the bubble interaction behaviour in gas-liquid two-phase flow system. For example, breakage and coalescence events produce very different bubble size distribution and then affect the interfacial interaction between the phases as well as the evolution of bubble size along two-phase flow system. It is well known that the solution including the population balance is much better than one using a single bubble size. However, there are very few experiment data, with well controlled initial bubble size distribution, available for validating the simulations. In order to investigate the bubble size effect on two-phase flow evolution and to provide a data set for developing the physical models to describe the bubble-induced turbulence effect and also for validating the code developed for predicting two-phase flow behaviour, a series of local parameter measurements were conducted using the five-sensor conductivity probe technique in air-water vertical-upward flow condition in which the initial bubble size is controlled by a specially designed bubble generator. The experimental results are analysed and discussed in this paper.

1. Bubble-Induced Turbulence Modelling

1.1 The concept proposed by Sato

In the k- ε turbulence model for a single-phase flow, the turbulence viscosity μ_T is defined as a relation between turbulent kinetic energy (k) and turbulent eddy dissipation rate (ε) by:

$$\mu_T = C_\mu \rho_f \frac{k^2}{\varepsilon} \tag{1}$$

where ρ_f is the liquid density and $C_{\mu} = 0.09$

For two-phase flow, the bubble-induced turbulence (BIT) was proposed by Sato [11] with considering an additional term into turbulent viscosity by

$$\mu_S = 0.6 \rho_f \alpha_g \left| \vec{u}_g - \vec{u}_f \right| \tag{2}$$

where α_g is the gas volume fraction, \vec{u}_g and \vec{u}_f are the gas and liquid velocity, respectively.

Hence, the standard k- ε turbulence model using Sato approach can be described as follows:

$$\frac{\partial(\alpha_f \rho_f k)}{\partial t} + \nabla \cdot \left(\alpha_f \rho_f \vec{u}_f k\right) = \nabla \cdot \left[\alpha_f \left(\mu + \frac{\mu_T}{\sigma_k}\right) \nabla k\right] + \alpha_f P - \alpha_f \rho_f \varepsilon \tag{3}$$

$$\frac{\partial(\alpha_f \rho_f \varepsilon)}{\partial t} + \nabla \cdot \left(\alpha_f \rho_f \vec{u}_f \varepsilon\right) = \nabla \cdot \left[\alpha_f \left(\mu + \frac{\mu_T}{\sigma_{\varepsilon}}\right) \nabla k\right] + \alpha_f \frac{\varepsilon}{k} \left(C_{\varepsilon 1} P - C_{\varepsilon 2} \rho_f \varepsilon\right) \tag{4}$$

$$\mu_{T} = C_{\mu} \rho_{f} \frac{k^{2}}{\varepsilon} + \mu_{S} = C_{\mu} \rho_{f} \frac{k^{2}}{\varepsilon} + 0.6 \rho_{f} \alpha_{g} |\vec{u}_{g} - \vec{u}_{f}|$$
(5)

The constants in the above equations have been chosen by optimizing the calculation results to fit a wide range of single-phase turbulent flows; nevertheless the same constant values are used in two-phase flows. The widely used values are follows [12]:

$$C_{\varepsilon 1} = 1.44, \ C_{\varepsilon 2} = 1.92, \ \sigma_k = 1.0, \ \sigma_{\varepsilon} = 1.3, \ C_{\mu} = 0.09$$

1.2 The concept of bubble-induced source for turbulence kinetic energy and its dissipation rate

The standard k- ε turbulence model, modelling the BIT via source terms Φ_k and Φ_{ε} , can be described as follows:

$$\frac{\partial(\alpha_f \rho_f k)}{\partial t} + \nabla \cdot \left(\alpha_f \rho_f \vec{u}_f k\right) = \nabla \cdot \left[\alpha_f \left(\mu + \frac{\mu_T}{\sigma_k}\right) \nabla k\right] + \alpha_f P - \alpha_f \rho_f \varepsilon + \alpha_f \Phi_k$$
 (6)

$$\frac{\partial(\alpha_{f}\rho_{f}\varepsilon)}{\partial t} + \nabla \cdot \left(\alpha_{f}\rho_{f}\vec{u}_{f}\varepsilon\right) = \nabla \cdot \left[\alpha_{f}\left(\mu + \frac{\mu_{T}}{\sigma_{\varepsilon}}\right)\nabla k\right] + \alpha_{f}\frac{\varepsilon}{k}\left(C_{\varepsilon 1}P - C_{\varepsilon 2}\rho_{f}\varepsilon\right) + \alpha_{f}\Phi_{\varepsilon}$$
(7)

$$\mu_T = C_\mu \rho_f \frac{k^2}{\varepsilon} \tag{8}$$

The bubble-induced source term Φ_k in turbulent kinetic energy equation (6) represents the interaction between the gas and liquid phase at the phasic interface. Most of BIT correlations that are found in the literature consider the work of the drag forces. In some correlations a contribution of non-drag forces is considered. The following expression for the bubble-induced source for turbulent kinetic energy is given by assuming that all friction work of a rising bubble is converted into turbulent kinetic energy:

$$\Phi_k = -\vec{F}_D \cdot \alpha_g |\vec{u}_g - \vec{u}_f| \tag{9}$$

where \vec{F}_D is the drag force, α_g is the gas volume fraction, \vec{u}_g is the gas velocity, and \vec{u}_f is the gas velocity.

Unfortunately, there is no theoretical justification in the literature for the source of turbulence eddy dissipation. Most of previous works correlated Φ_{ε} with Φ_k and the relaxation time τ_{BIT} which is calculated on a dimensional background.

The bubble induced source for turbulence eddy dissipation in equation (7) is obtained as below [13]:

$$\Phi_{\varepsilon} = C_{\varepsilon 3} \tau_{RIT}^{-1} \Phi_{k} \tag{10}$$

Table 1 shows a summary of the development of Φ_k and Φ_{ε}

Table 1: Bubble Induced Turbulence source terms

	$oldsymbol{arPhi}_k$	$oldsymbol{\Phi}_{arepsilon}$		
Authors	Work of drag forces	Other contributions		
Morel (1997)	$\frac{1}{\alpha_f} A_D u_r \left(A_D = \frac{3}{4} \alpha_g C_D \frac{ \vec{u}_r ^2}{d_s} \right)$	$\frac{1+2\alpha_g}{2\alpha_f} \left(\frac{D_g \vec{u}_g}{Dt} - \frac{D_f \vec{u}_f}{Dt} \right) \cdot \vec{u}_r$	-	
Pfleger and Becker (2001)	$C_k A_D u_r \ (C_k = C_{\varepsilon_1})$	None		
Troshko and Hassan (2000)	$\frac{1}{\alpha_{_f}} \big A_{_D} \big\ u_r \big $	None		
Lahey (2005)	$C_{p}(1+C_{D}^{4/3})\alpha_{g}\frac{\left \bar{u}_{r}\right ^{3}}{d_{s}}$ $\left(C_{p}=0.25\right)$	None	$C_{arepsilon 2} au_{ extit{BIT}}^{-1} oldsymbol{arPhi}_k \ \left(au_{ extit{BIT}}^{-1} = rac{arepsilon}{k} ight)$	
Star-CD	$\left \frac{3}{4} \frac{C_D}{d_B} \frac{\alpha_g}{\alpha_f} \vec{u}_r \left\{ 2(C_t - 1)k - \frac{v_c^T}{\alpha_g \alpha_f \sigma_\alpha} u_r \cdot \nabla \alpha_g \right\} \right.$	None	$\frac{3}{2}\frac{C_D}{d_B}\frac{\alpha_g}{\alpha_f}\Big \vec{u}_r\Big (C_t-1)\varepsilon$	

2. The effect of BIT on the interfacial area transport prediction

The IATE has been used by various studies for two-phase flow such as Ishii et al. [14], Hibiki and Ishii [15], Yao and Morel [16], and Bae et al. [2], [3]. For the adiabatic gas-liquid flow condition, the basic form of governing equation is as follows:

$$\frac{\partial a_i}{\partial t} + \nabla \cdot \left(a_i u_g \right) = -\frac{2}{3} \frac{a_i}{\rho_a} \frac{d\rho_g}{dt} + \phi_{co} + \phi_{bk} \tag{11}$$

The first term on the right-hand side of Eq. (11) is the term for a bubble size variance due to a pressure drop. The second and the third term mean the variance of interfacial area concentration (IAC) by a coalescence and break-up, respectively. In the adiabatic bubbly flow, the coalescence by a random collision (RC) and the break-up by a turbulent impact (TI) are considered as dominant terms for the mechanistic models of ϕ_{co} and ϕ_{bk} . Unlike other models suggested by Wu et al. [17] and Hibiki and Ishii [15], Yao and Morel's model considers the free-travelling time (T_{cf} for a coalescence and T_{bf} for a breakup) and the interaction time (T_{ci} for a coalescence and T_{bi} for a breakup) of bubbles separately. This approach has improved the capability of predicting IAC by mechanistically modelling the coalescence or breakup process. Recently, a commercial CFD-code analysis of Cheung et al [7] represented that the model of Yao and Morel showed a better agreement for an air/water adiabatic flow. Hence, the Yao and Morel's models for coalescence and breakup source term have been chosen for analysing of the EAGLE code. The detailed models are given as follows:

The 14th International Topical Meeting on Nuclear Reactor Thermalhydraulics, NURETH-14 Toronto, Ontario, Canada, September 25-30, 2011

$$\phi_{RC} = -\frac{1}{3\psi} \left(\frac{\alpha}{a_i}\right)^2 \cdot \frac{1}{2} \frac{\eta_c n}{T_c} = -\frac{1}{3\psi} \left(\frac{\alpha}{a_i}\right)^2 \cdot \frac{1}{2} \frac{\eta_c n}{T_{cf} + T_{ci}}$$

$$= -\frac{1}{3\psi} \left(\frac{\alpha}{a_i}\right)^2 \cdot K_{c1} \frac{\varepsilon^{1/3} \alpha^2}{D_b^{11/3}} \cdot \frac{1}{g(\alpha) + K_{c2} \alpha \sqrt{We/We_c}} \cdot \exp\left(-K_{c3} \sqrt{\frac{We}{We_c}}\right)$$
(12)

$$\phi_{TI} = \frac{1}{3\psi} \left(\frac{\alpha}{a_i}\right)^2 \cdot \frac{\eta_b n}{T_b} = \frac{1}{3\psi} \left(\frac{\alpha}{a_i}\right)^2 \cdot \frac{\eta_b n}{T_{bf} + T_{bi}}$$

$$= \frac{1}{3\psi} \left(\frac{\alpha}{a_i}\right)^2 \cdot K_{b1} \frac{\varepsilon^{1/3} \alpha (1 - \alpha)}{D_b^{11/3}} \cdot \frac{1}{1 + K_{b2} (1 - \alpha) \sqrt{We/We_c}} \cdot \exp\left(-\frac{We_c}{We}\right)$$
(13)

$$We = \frac{2\rho_f (\varepsilon D_b)^{2/3} D_b}{\sigma} \tag{14}$$

where ψ is the bubble shape factor, $1/36\pi$ for a spherical bubble, and η and n are the interaction efficiency of neighbouring bubbles and bubble number density, respectively. We is the Weber number and ε is the turbulent energy dissipation rate which can be obtained from the standard k- ε turbulence model, $g(\alpha)$ is a modification factor defined as $1-(\alpha/\alpha_{\rm max})^{1/3}$, and the coefficients in the equations are $K_{c1}=2.86$, $K_{c2}=1.922$, $K_{c3}=1.017$, $We_c=1.24$, $\alpha_{\rm max}=0.52$, $K_{b1}=1.6$, $K_{b2}=0.42$. The detailed structure of EAGLE code can be found in [2], [3].

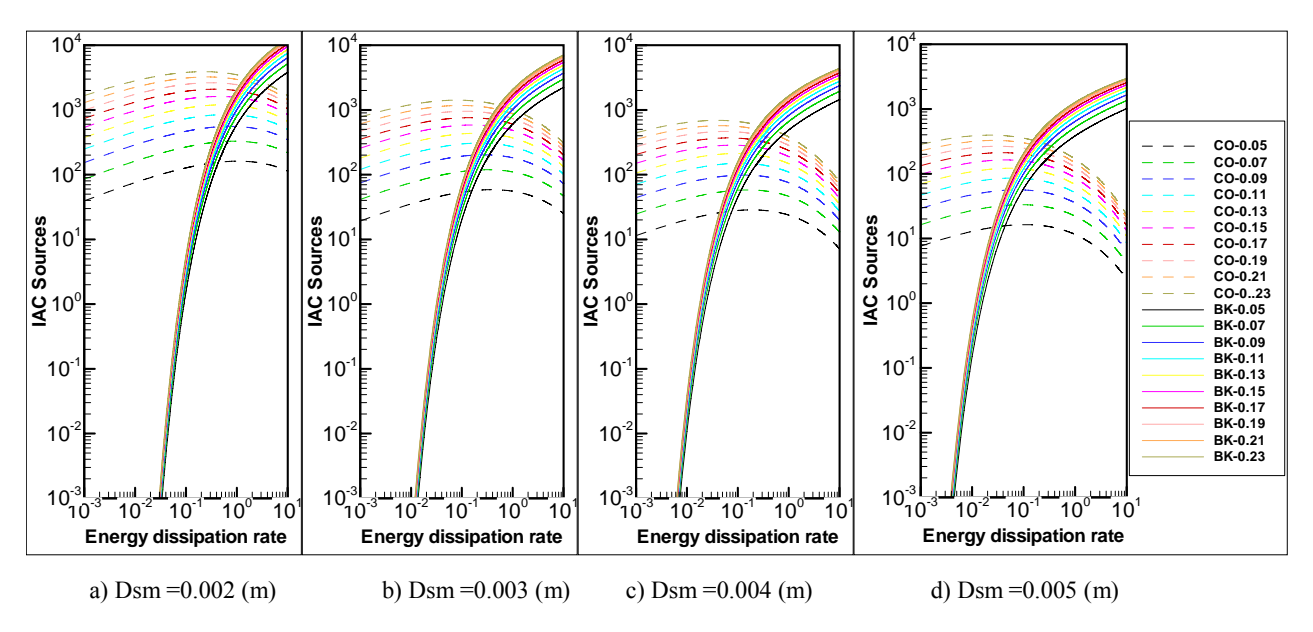


Fig 1: The dependence of source and sink terms on turbulent energy dissipation rate

A parametric study has been carried out in order to investigate the sensitivity of coalescence and breakup source terms on the turbulence energy dissipation rate ε . Typical results are shown in Fig. 1. As can be seen, the difference between bubble source and sink terms strongly depends on the turbulence energy dissipation rate. As the value of ε is decreased, the

bubble coalescence sink term is still high and not changed so much, whereas the bubble breakup source term is rapidly decreased to zero. It does mean that the underestimation of ε could easily lead to the overestimation of bubble size. Therefore, the turbulence models for bubbly two-phase flows should be modelled correctly by taking into account the effect of bubble induced turbulence.

In the present study, two common modelling concepts of BIT are implemented in the EAGLE code with the standard k-\varepsilon turbulence model for liquid phase. One of the most challenging steps of the modelling is to select a proper experimental data for model development and validation. The local void fraction, interfacial area concentration, mean bubble diameter, phase velocities and turbulent parameters are indispensable for validating the models. The experimental data of Hibiki et al. [1] for vertical upward air-water flows in a round tube with an inner diameter of 50.8 mm under atmospheric pressure were selected for the two-phase flow analysis. This data set provides a lot of useful local parameters, especially the turbulent intensity, which had been measured at 15 points in the radial distribution as well as at three axial locations of z/D = 6.00, 30.3 and 53.5, by using double-sensor probes and the hot film probes. The uncertainty analysis can be found in [1]. The typical test conditions selected for this study are listed in Table 2. The Case 1 and 2 with low superficial liquid velocity, and the case 3 with high superficial liquid velocity were chosen. In order to give a meaningful comparison between CFD prediction and experiment, numerical uncertainty should be first estimated, especially the grid sensitivity. Several calculations with different refinements of grid size were performed in cylindrical coordinate. Number of control volumes was 50, 80, 150 in axial direction and 10, 12, 14, 16, 18, 20, 22 in radial direction. Fig. 2 presents results of grid sensitivity analysis with Case 1 simulation. As shown in this figure, starting from 20 nodes in radial direction, the results essentially do not vary. There is no significant change as the number of axial nodes is changed. It should be noted that the EAGLE code adopted wall function laws, therefore the wall y+ value should be greater than 30. It was found that this condition is satisfied in all cases.

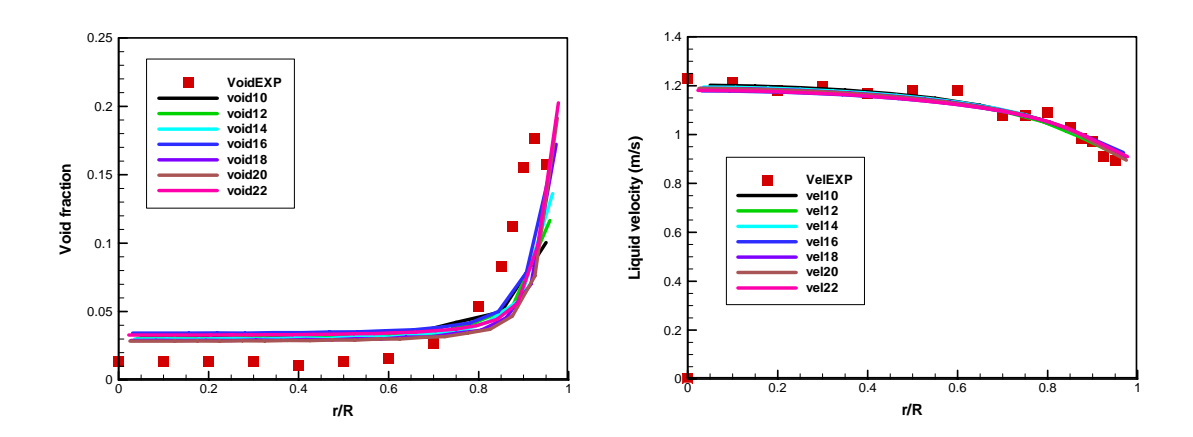


Fig 2: Grid sensitivity calculation

The local parameters at the axial location of z/D = 6.00 were selected as initial conditions in our study with the following assumptions about the relation between turbulent intensity and turbulent parameters:

The 14th International Topical Meeting on Nuclear Reactor Thermalhydraulics, NURETH-14 Toronto, Ontario, Canada, September 25-30, 2011

$$\begin{cases} k = \frac{1}{2} \left(u^2 + \frac{1}{2} u^2 + \frac{1}{2} u^2 \right) = u^2 \\ \varepsilon = \frac{\left(u^2 / 2 \right)^{3/2}}{d_s} \\ i = \frac{u}{U_{mean}} \end{cases}$$
 (15)

where k, ϵ , u, i, d_s are liquid turbulent kinetic energy, turbulent energy dissipation rate, velocity fluctuation, turbulent intensity and bubble mean diameter, respectively. Following Yun's approach [18], the assumption for turbulence kinetic energy in equation (15) is made based on three-dimensional turbulence structure measurements of Wang [19] in which the turbulence anisotropy due to the presence of the gas phase has been found. The axial kinetic energy component is approximately two times larger than the lateral kinetic energy component.

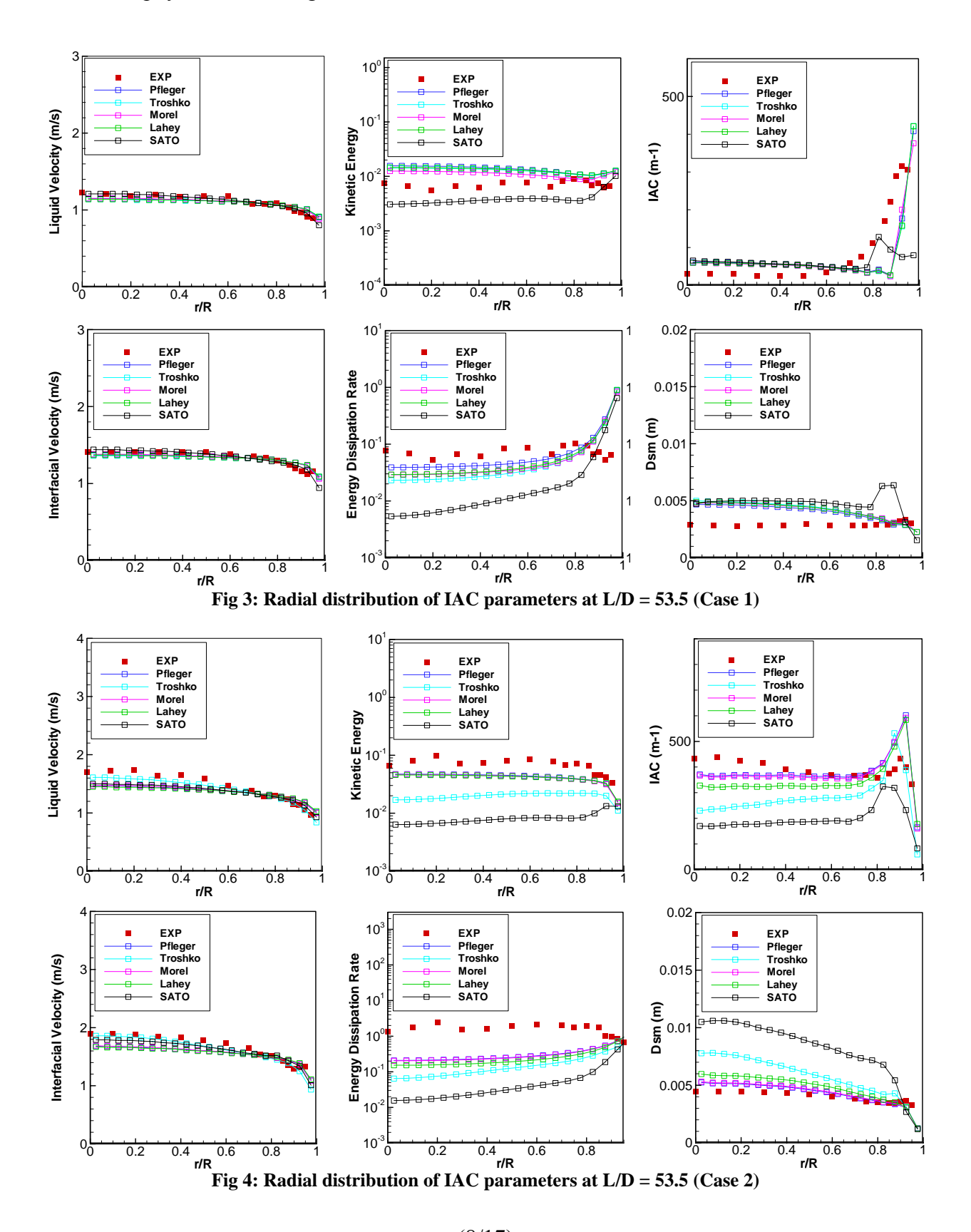
After these calculations, the analysis was conducted within a grid composed of 20 (radial) x 80 (axial) axisymmetric cells in a cylindrical coordinate. A zero-gradient condition was taken into account at the outlet boundary. Various constitutive models of two-phase flow have been analysed and validated in [2],[3]. In this study, the interfacial drag force model of Ishii & Zuber (1979), the turbulent dispersion force model of Burns (2004), the lift force model of Ishii (2006), and the wall lubrication force model of Antal (1991) were adopted.

Table 2: Test cases for assessment

	Case 1	Case 2	Case 3
j _f (m/s)	0.986	0.986	5.00
j _g (m/s)	0.0473	0.321	0.245

Figures 3 to 5 represent the analysis results of local parameters at the axial location L/D =53.5 for the cases 1 to 3, respectively. These figures compare the results of various bubbleinduced turbulence models. As shown in the figures, the prediction results of all bubble-induced turbulence models for superficial liquid velocity and superficial gas velocity profile are almost similar and agree well with the experimental data. For the condition of low superficial liquid velocity in the case 1 and 2, the Sato's model underestimates the energy dissipation rate in comparison with the bubble-induced source models. Therefore, from Fig. 1, the unbalance between sink and source terms in Sato's model is bigger than that of BIT models and it resulted in the underestimation of IAC and the overestimation of bubble mean diameter as depicted in Fig. 3 and Fig. 4. The void fraction in the case 1 is much smaller than that of the case 2, hence the deviation in the case 1 is smaller than that of the case 2. Among bubble-induced source models, the prediction of Pfleger's model shows the best agreement with the experimental data. For the condition of high superficial liquid velocity in the case 4, the prediction results of all bubble-induced turbulence models for turbulent energy dissipation rate are almost the same. However, they underestimate the bubble mean diameter and overestimated the IAC as depicted in Fig. 5. It might be explained in such way that the turbulent energy generation and dissipation rate near the wall boundary are very large in high liquid flow condition due to large gradient of liquid velocity. As shown in Fig. 1, the breakup process is dominant in this case because the turbulent energy dissipation is very high. It can be concluded that the prediction of IAC

parameters is strongly depend on the performance of turbulence models in two-phase flow as well as the physical modelling of source terms in IATE.



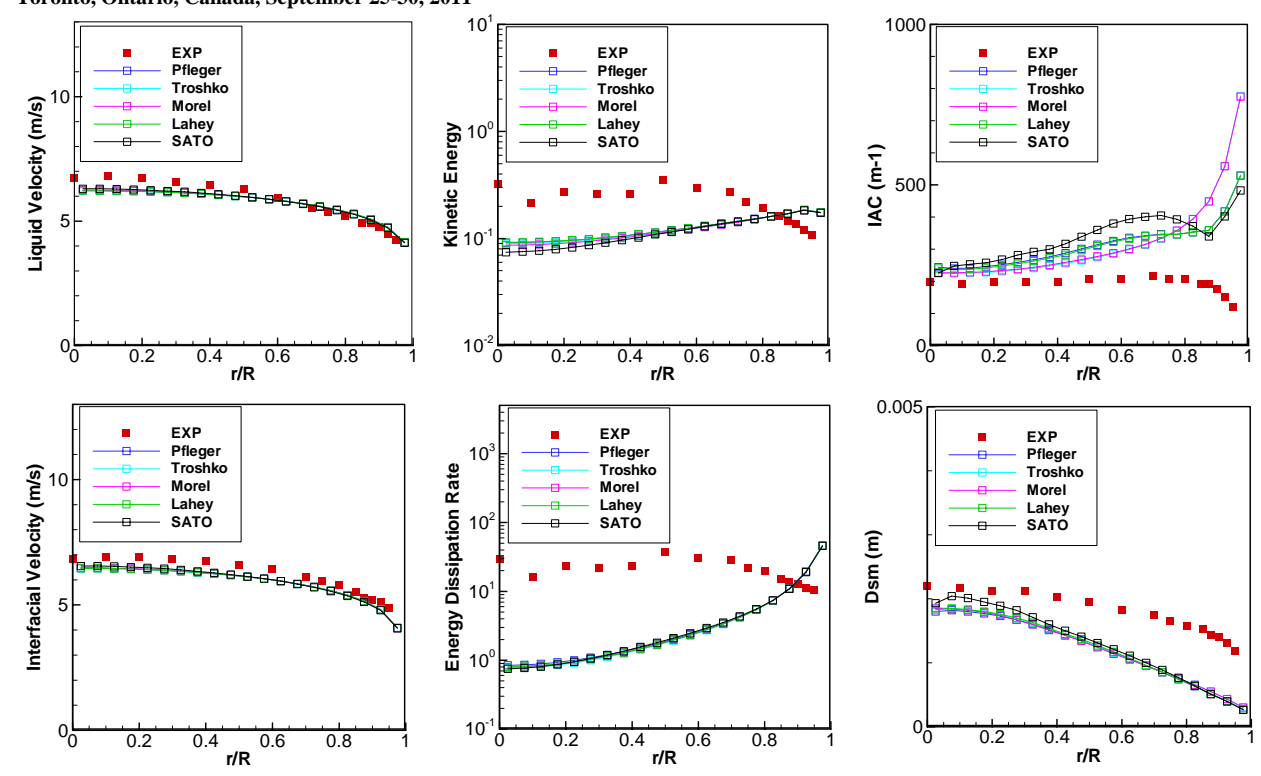


Fig 5: Radial distribution of IAC parameters at L/D = 53.5 (Case 3)

3. The effect of bubble size on the interfacial area transport prediction

The vertical air-water loop (VAWL) has been used for investigating the transport phenomena of two-phase flow at Korea Atomic Energy Research Institute (KAERI). A schematic diagram of the test facility is shown in Fig. 6a. Further details about test facility as well as the uncertainty of measurement can be found in [10], [20]. The transport phenomena of void fraction and interfacial area concentration are measured by using five-sensor conductivity probe method [10]. With this method, the data for void fraction and interfacial area concentration are obtained and classified into two groups, that is, the small spherical bubble group and the cap/slug one.

Although the experimental data of Hibiki et al. [1] gave a comprehensive set of local IAC parameter measurements, the initial condition was not controlled. They demonstrated that the initial bubble size increased with increasing the gas flow rate, whereas it decreased with increasing the liquid flow rate. It should be recalled that the local distribution of phases are strongly depend on an initial condition. In our experimental facility, the initial bubble size is controlled by a specially designed bubble generator which was depicted in Fig. 6b [20]. The main water flow forms at both sides of the bubble generator. The bubble generator is securely connected to the test section through piping. Some of the main water is injected into the bubble generator. Air is also injected into the central region of the bubble generator through air chamber consisting of 16 holes with 1.5 mm in diameter and mixed with the injected water and enters the test section. The generated bubble size is determined by the degree of the turbulence that is created by the injected water and airflow as well as the size of the nozzles inside the bubble generator. Hence, this bubble generator can control the bubble size by changing the bypass flow

rate without changing the main water flow or the air flow. The loop temperature was kept at a constant temperature (30°C) by a preheater and a cooler. The loop is pressurized to 2 bars to avoid the effect of the difference in hydrostatic heads along the channel on the bubble growth, and the system pressure is automatically maintained and controlled by a special valve installed at the top of the water storage. The local measurements using the five-sensor conductivity probe and bidirectional flow tube were performed at three axial locations of z/D = 12.2, 42.2, and 100.7. The accuracy of local measurements is assured by integrating the local flow parameters over the flow channel and comparing with the area-averaged measurements by Impedance Void Meter (IVM), gas and liquid flow meters. The photographic method using high speed camera was applied in order to investigate the interaction mechanism between phases. The test flow conditions for low superficial liquid velocity are tabulated in Table 3. Tables 4 and 5 show the results of the uncertainty analysis for the probe parameters and the averaged parameters with 95% confidence. The basic equations for the uncertainty analysis are summarized in [10]

For $\langle j_f \rangle = 0.5$ m/s, $\langle j_g \rangle = 0.044$ m/s, a well-developed wall peaking void fraction profile was observed with the bypass ratio of 0.9 at the bubble generator even at the first measuring station, whereas a well-developed core peaking void fraction profile was observed with the bypass ratio of 0.1 (Fig. 7). In the former case, the initial bubble size was uniformly distributed so that there is no appearance of large bubble and then the bubble coalescence due to the wake entrainment mechanism is unlikely to occur. The bubbles are small and they have tendency to migrate toward the wall resulting in wall peaking void fraction profile as previously achieved by many researchers. Further information regarding the core peaking and wall peaking void fraction profile can be found in Song et al. [21].

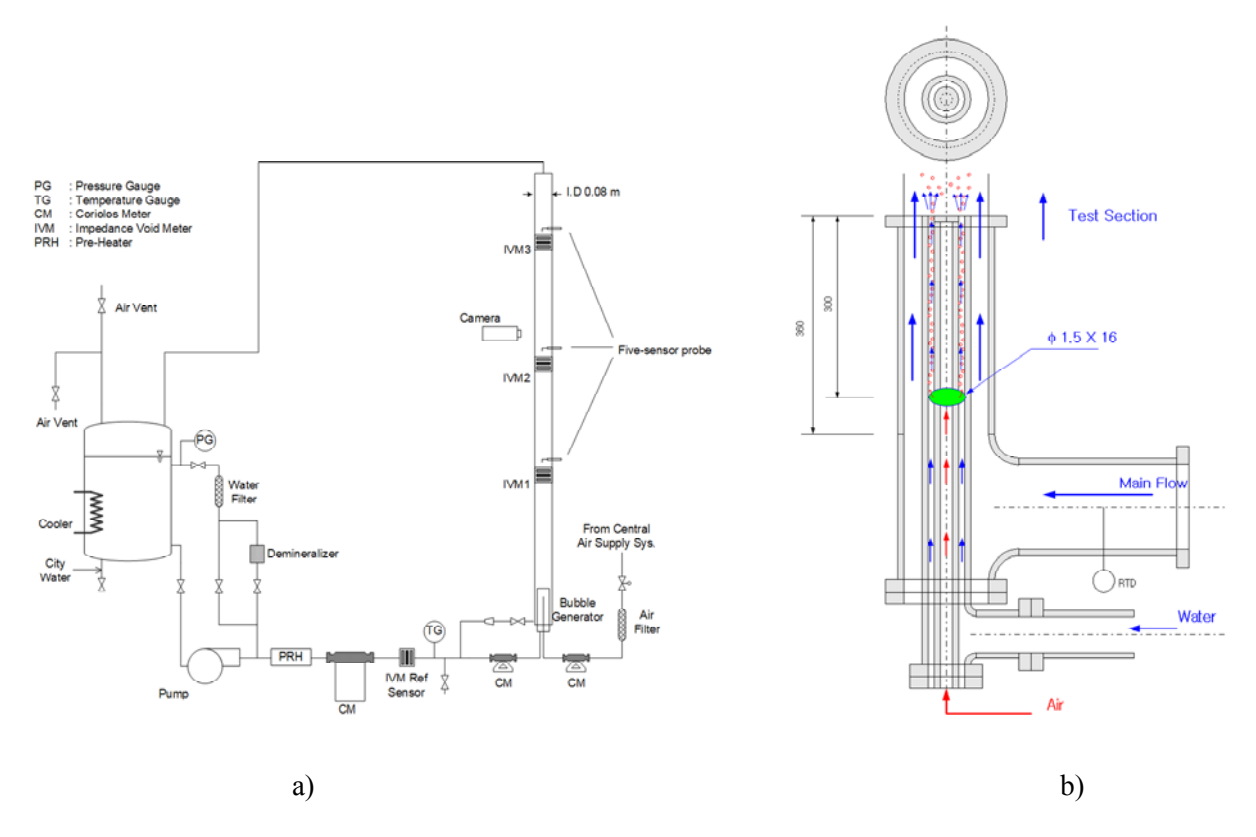


Fig 6: Test facility and bubble generator

Table 3: Test matrix

Test	<j<sub>f></j<sub>	< j g>	Bypass ratio -		Pressure		
	(m/s)	(m/s)		Bubble Group (I)	Bubble Group (II)	Total	(bar)
Run01	0.5	0.044	0.1		•		2
Run02	0.5	0.044	0.9				2
Run03	0.5	0.148	0.1	•	•	•	2
Run04	0.5	0.148	0.9	0	0	0	2
Run05	0.5	0.288	0.1	*	•	•	2
Run06	0.5	0.288	0.9	♦	♦	\Diamond	2

Table 4: Uncertainty analysis of probe parameters

	Void fraction (2 nd elevation) %	Void fraction (3 rd elevation) %	IAC (2 nd elevation) %	IAC (3 rd elevation) %	D _{sm} (2 nd elevation) %	D _{sm} (3 rd elevation) %	Bubble frequency (2 nd elevation) %	Bubble frequency (3 rd elevation) %
Run01	3.2	3.2	3.5	3.2	5.1	4.8	1.9	1.8
Run02	2.3	2.3	2.6	2.4	3.6	3.5	1.3	1.3
Run03	3.8	2.9	4.0	3.5	5.8	5.1	2.1	1.6
Run04	1.5	2.8	1.7	3.0	2.4	4.2	0.8	1.7
Run05	5.0	2.9	4.5	3.5	6.8	5.1	2.6	1.6
Run06	3.0	2.8	3.3	3.4	4.6	5.0	1.9	1.7

Table 5: Uncertainty analysis of averaged parameters

	Pressure (1 st elevation) %	Pressure (2 nd elevation) %	Pressure (3 rd elevation) %	Void fraction (1 st elevation) (IVM) %	Void fraction (2 nd elevation) (IVM) %	Void fraction (3 rd elevation) (IVM) %	Liquid Flow %	Gas Flow %	Temp %
Run01	0.4	0.4	0.6	14.1	15.2	16.7	1.7	28.9	1.7
Run02	0.4	0.4	0.6	11.0	12.0	13.6	1.7	28.0	1.7
Run03	0.4	0.4	0.6	4.8	5.3	6.1	1.7	8.7	1.7
Run04	0.4	0.4	0.6	3.3	3.7	5.1	1.7	9.3	1.7
Run05	0.4	0.4	0.6	2.6	3.1	4.0	1.7	4.4	1.7
Run06	0.4	0.4	0.6	1.7	2.4	3.6	1.7	4.4	1.7

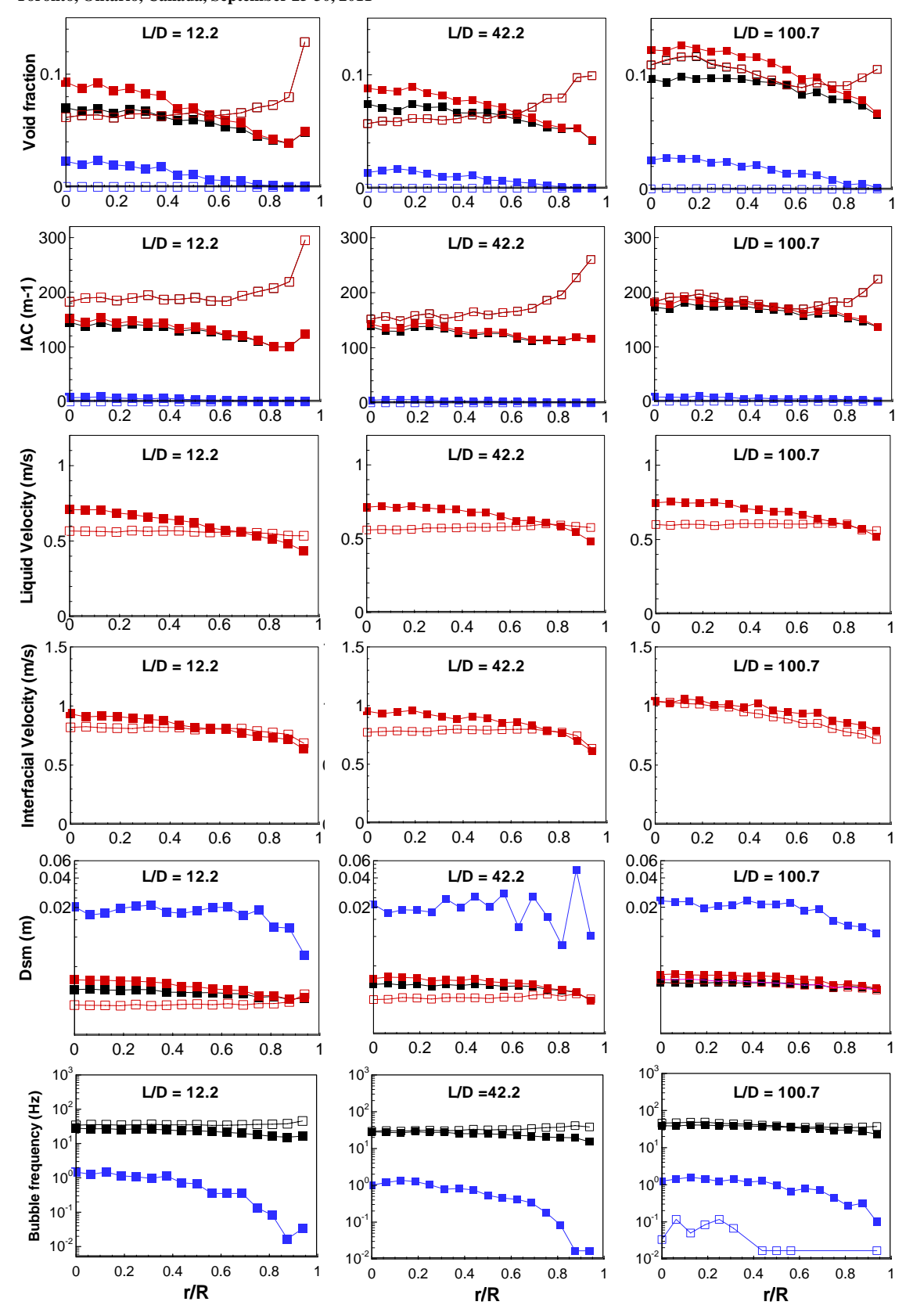


Fig 7: Experimental results of Run01 and Run02

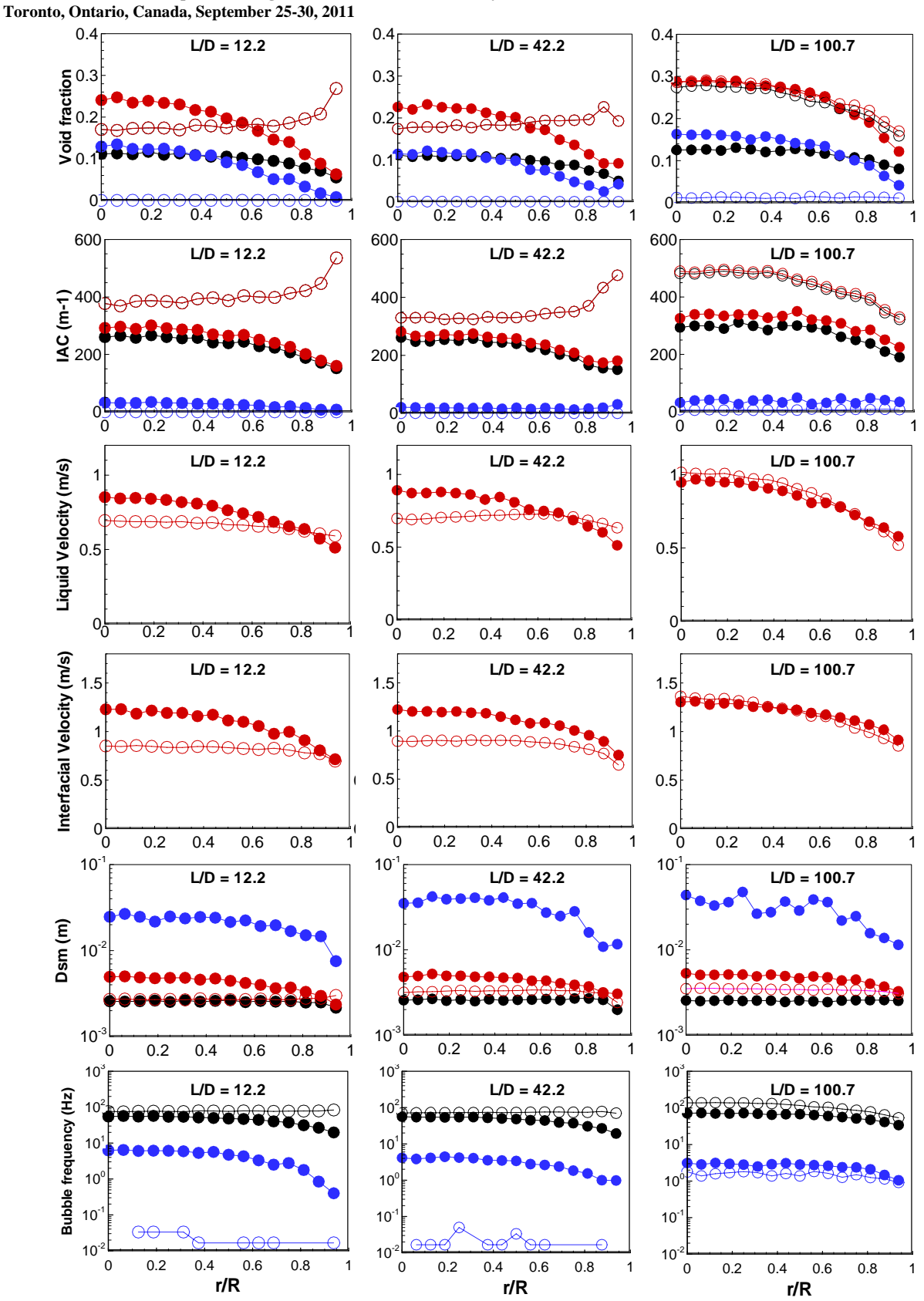


Fig 8: Experimental results of Run03 and Run04

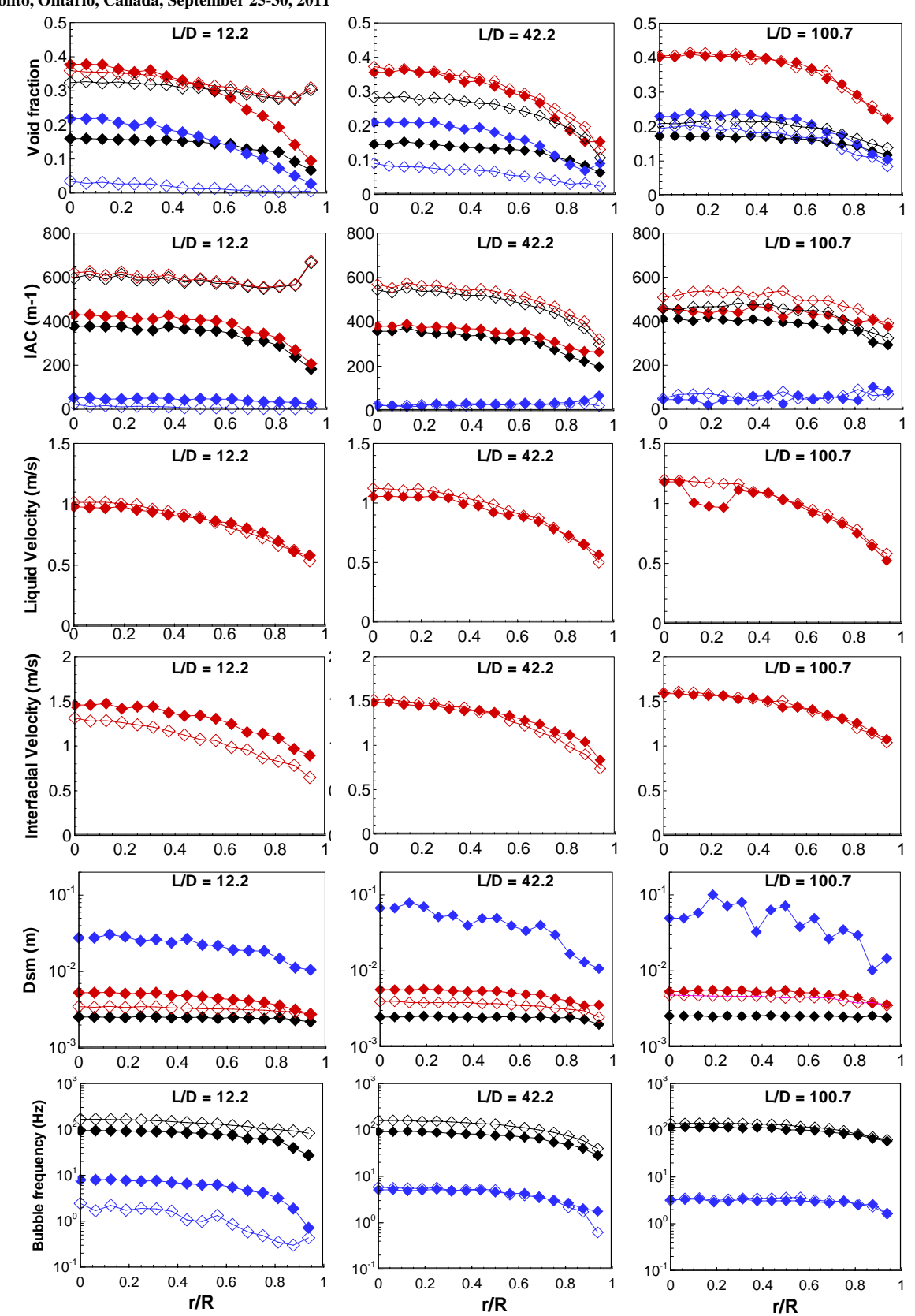


Fig 9: Experimental results of Run05 and Run06

The bubble size became gradually increased along the flow direction by the expansion due to the axial pressure reduction, and then the large bubble had tendency to migrate toward the centre of channel at the second and the third measuring elevations. In the latter case, large bubbles were even formed at the first measuring point. Therefore, the bubble coalescence would be enhanced because of wake entrainment effect. It should be noted that the gas and liquid profiles of the former case are flatter than those of the latter case.

As shown in [1], in low void fraction cases, the bubble coalescence due to the bubble collision driven by liquid turbulence as well as the bubble breakup due to turbulent impact might be unlikely occur because of a small liquid turbulence and a relatively large distance between bubbles. In our experiments, the same results were obtained even in case of high void fraction with well-controlled value of initial bubble size at the first and second measuring elevations (L/D = 12.2 and 42.2) (Fig. 8, 9). However, at the third measuring elevation (L/D = 100.7), the frequency of large bubble in case of low and high bypass ratio are almost the same. It was observed that the effect of bubble expansion due to pressure reduction in latter case is dominant resulting in the tendency of large bubble migration toward the centre of flow channel without coalescing with smaller bubbles, whereas in the former case, both the effect of bubble expansion and coalescence due to wake entrainment are dominant. It can be seen in the contribution of two bubble group on interfacial concentration. It should be noted that the experiment was performed at atmospheric pressure condition. The investigation is needed to be done in higher pressure condition. It is interesting that our experimental data provided the information on IAC, Sauter mean diameter, and frequency of two bubble groups which are very useful for the poly-dispersed bubble approach in two-phase flow.

4. Conclusions

Analysis results presented in this paper show that the prediction of the interfacial area transport equation strongly depends on the correct modelling of turbulent parameters in two-phase flow, especially the turbulent kinetic energy dissipation and its scale distribution. The implementation of bubble-induced turbulence models with source term approach can improve the prediction. However, further improvement of turbulence modelling, as well as IATE source terms are still required. The initial bubble size condition has also a big influence on the interaction mechanism between phases. In relation to the investigation of initial bubble size effect, local measurements of void fraction, interfacial area concentration, Sauter mean diameter, and bubble frequency using five-sensor probe method as well as the liquid velocity using local bi-directional flow transmitter were performed for the bubbly flows with well-controlled bubble size. Compared with the experimental data of Hibiki et al. [1], our data is very unique considering the initial bubble size effect and is very useful with capability of two-group of bubble information which is indispensable for two-group IATE development.

ACKNOWLEGEMENT

This work was supported by the Nuclear Research & Development Program of the National Research Foundation (NRF) grant funded by the Korean government (MEST). (grant code: M20702040003-08M0204-00310). The authors are thankful to Dr. Byoung-Jo Yun for his advice and discussion related to this work.

REFERENCES

- [1] T. Hibiki, M. Ishii, Z. Xiao, "Axial interfacial area transport in bubbly flow systems", Int. J. Heat and Mass Transfer, 44, 2001, pp. 1869-1888.
- [2] B.U. Bae, H.Y. Yoon, D.J. Euh, C.-H. Song and G.C. Park, "Computational Analysis of a Subcooled Boiling Flow with a One-group Interfacial Area Transport Equation", Journal of Nuclear Science and Technology, Vol. 45, No. 4, 2008, pp.341-351
- [3] B.U. Bae, B.J. Yun, H.Y. Yoon, C.-H. Song, G.C. Park, "Analysis of subcooled boiling flow with one-group interfacial area transport equation and bubble lift-off model", Nuclear Engineering and Design, Vol. 240, Issue 9, 2010, pp. 2281-2294.
- [4] M. Ishii, "Thermo-fluid dynamic theory of two-phase flow", Direction des Etudes et Researches d'Electricite de France, Paris, France (1975).
- [5] M. Ishii, T. Hibiki, "Thermo-fluid dynamics of two-phase flow", Springer Inc., New York, U.S., 2006.
- [6] C.-H. Song, D.J. Euh, B.J. Yun, I.-C. Chu, B.U. Bae, S.K. Chang, W.P. Baek, "KAERI Research Activities for Interfacial Area Transport in Two-Phase Flow", Transactions of the American Nuclear Society, Vol. 103, 2010, pp. 921-922.
- [7] S.C.P. Cheung, G. H. Yeoh, J. Y. Tu, "On the modeling of population balance in isothermal vertical bubbly flows-Average bubble number density approach", Chemical Engineering and Processing, 46, 2007, pp. 742-756.
- [8] S. Al Issa, D. Lucas, "Two phase flow 1D turbulence model for poly-disperse upward flow in a vertical pipe", Nuclear Engineering and Design, Vol.239, 2009, pp.1933-1943.
- [9] B.J. Yun, A. Splawski, S. Lo, and C.-H. Song, "Evaluation of One-Group Interfacial Area Transport Equation for the Air/water Flow Condition with CFD Code", Transactions of the American Nuclear Society, Vol. 103, 2010, pp. 941-942.
- [10] D.J. Euh, B.J. Yun, C-.H. Song, T.S. Kwon, M.K. Chung, U.C. Lee, "Development of the Five Sensor Conductivity Probe Method for the Measurement of Interfacial Area Concentration", Nuclear Engineering and Design, Vol 205, 2001, pp. 35-51.
- [11] Y. Sato and K. Sekoguchi, "Liquid velocity distribution in two-phase bubble flow", Int. J. Multiphase Flow, Vol.2, 1975, pp. 79-95.
- [12] B. E. Launder and D. B. Spalding, "The numerical computation of turbulent flows", Computer Methods in Applied Mechanics and engineering, Vol.3, 1974, pp.269-289.
- [13] E. Krepper, M. Schmidte, D. Lucas, "Modeling of Turbulence in Bubbly Flows", Proceedings of the 7th International Conference on Multiphase (ICMF-2010), May.30-June 4, 2010, Tampa, Florida, USA.
- [14] M. Ishii, S. Kim, J. Uhle, "Interfacial area transport equation: model development and benchmark experiments", International Journal of Heat and Mass Transfer, Vol. 45(15), 2002, pp. 3111-3123.

- [15] T. Hibiki, M. Ishii, "Development of one-group interfacial area transport of vertical bubbly flows", Int. J. Heat and Mass Transfer, 45, 2002, pp. 2351-2372
- [16] W. Yao, C.Morel, "Volumetric interfacial area prediction in upward bubbly two-phase flow", Int. J. Heat and Mass Transfer, 47, 2004, pp.307-328.
- [17] Q. Wu, S. Kim, M. Ishii, et al, "One-group interfacial area transport in vertical bubbly flow", Int. J. Heat and Mass Transfer, 41, 1998, pp. 1103-1112.
- [18] B.J. Yun, "Assessment of Subcooled Boiling Flow with Mechanistic Bubble Size Model", Technical meeting at KAERI, Daejeon, Korea (2010)
- [19] S. K. Wang, S. J. Lee, O. C. Jones JR, and R. T. Lahe JR, "3-D Turbulence structure and phase distribution measurements in bubbly two-phase flows", Int. J. Multiphase Flows 13, 1987, pp. 327-343.
- [20] C-.H. Song, M.K. Chung, H.C. No, "Measurements of void fraction by an improved multichannel conductance void meter", Nuclear Engineering and Design, Vol 184, 1998, pp. 269-285.
- [21] C-.H. Song, H.C. No, M.K. Chung,. "Investigation of bubble flow developments and its transition based on the instability of void fraction wave". Int. J. Multiphase Flow 21, 1995, pp. 381-404.